Article

Focal adhesion features during myofibroblastic differentiation are controlled by intracellular and extracellular factors

DUGINA, Vera, *et al*.

Abstract

Transforming growth factor beta (TGFbeta), the most established promoter of myofibroblast differentiation, induces ED-A cellular fibronectin and alpha-smooth muscle actin expression in fibroblastic cells in vivo and in vitro. ED-A fibronectin exerts a permissive action for alpha-smooth muscle actin expression. A morphological continuity (called fibronexus), a specialized form of focal adhesion, has been described between actin stress fibers that contain alpha-smooth muscle actin, and extracellular fibronectin, which contains the ED-A portion, in both cultured fibroblasts and granulation tissue myofibroblasts. We have studied the development of these focal adhesions in TGFbeta-treated fibroblasts using confocal laser scanning microscopy, three-dimensional image reconstruction and western blots using antibodies against focal adhesion proteins. The increase in ED-A fibronectin expression induced by TGFbeta was accompanied by bundling of ED-A fibronectin fibers and their association with the terminal portion of alpha-smooth muscle actin-positive stress fibers. In parallel, the focal adhesion size was importantly increased, [...]

Reference

DUGINA, Vera, *et al*. Focal adhesion features during myofibroblastic differentiation are controlled by intracellular and extracellular factors. *Journal of cell science*, 2001, vol. 114, no. Pt 18, p. 3285-3296

PMID : 11591817

Focal adhesion features during myofibroblastic differentiation are controlled by intracellular and extracellular factors

Vera Dugina[1], Lionel Fontao[2], Christine Chaponnier[2], Jury Vasiliev[1] and Giulio Gabbiani[2,*]

[1]Moscow State University, 119899 Moscow, Russia
[2]Department of Pathology, CMU, University of Geneva, 1 rue Michel-Servet, 1211 Geneva 4, Switzerland
*Author for correspondence (e-mail: giulio.gabbiani@medecine.unige.ch)

Accepted 7 June 2001
Journal of Cell Science 114, 3285-3296 © The Company of Biologists Ltd

SUMMARY

Transforming growth factor β (TGFβ), the most established promoter of myofibroblast differentiation, induces ED-A cellular fibronectin and α-smooth muscle actin expression in fibroblastic cells in vivo and in vitro. ED-A fibronectin exerts a permissive action for α-smooth muscle actin expression. A morphological continuity (called fibronexus), a specialized form of focal adhesion, has been described between actin stress fibers that contain α-smooth muscle actin, and extracellular fibronectin, which contains the ED-A portion, in both cultured fibroblasts and granulation tissue myofibroblasts. We have studied the development of these focal adhesions in TGFβ-treated fibroblasts using confocal laser scanning microscopy, three-dimensional image reconstruction and western blots using antibodies against focal adhesion proteins. The increase in ED-A fibronectin expression induced by TGFβ was accompanied by bundling of ED-A fibronectin fibers and their association with the terminal portion of α-smooth muscle actin-positive stress fibers. In parallel, the focal adhesion size was importantly increased, and tensin and FAK were neoexpressed in focal adhesions; moreover, vinculin and paxillin were recruited from the cytoplasmic pool into focal adhesions. We have evaluated morphometrically the length and area of focal adhesions. In addition, we have evaluated biochemically their content of associated proteins and of α-smooth muscle actin after TGFβ stimulation and on this basis suggest a new focal adhesion classification, that is, immature, mature and supermature.

When TGFβ-induced α-smooth muscle actin expression was blocked by soluble recombinant ED-A fibronectin, we observed that the fragment was localised into the fibronectin network at the level of focal adhesions and that focal adhesion supermaturation was inhibited. The same effect was also exerted by the ED-A fibronectin antibody IST-9. In addition, the antagonists of actin-myosin contractility BDM and ML-7 provoked the dispersion of focal adhesions and the decrease of α-smooth muscle actin content in stress fibers of pulmonary fibroblasts, which constitutively show large focal adhesions and numerous stress fibers that contain α-smooth muscle actin. These inhibitors also decreased the incorporation of recombinant ED-A into fibronectin network. Our data indicate that a three-dimensional transcellular structure containing both ED-A fibronectin and α-smooth muscle actin plays an important role in the establishment and modulation of the myofibroblastic phenotype. The organisation of this structure is regulated by intracellularly and extracellularly originated forces.

Key words: α-Smooth muscle actin, ED-A fibronectin, Wound healing, Stress fibers, Confocal microscopy

INTRODUCTION

Focal adhesions (FAs) link matrix-attached transmembrane integrin receptors to actin cytoskeleton via a complex of anchoring proteins (Critchley, 2000; Geiger et al., 1995; Jockusch et al., 1995; Yamada and Geiger, 1997). Two stages in FA formation and maturation have been identified: formation of initial or immature FAs (Bershadsky et al., 1985; Izzard, 1988; Izzard and Lochner, 1980; Izzard and Izzard, 1987), also called focal complexes, and maturation of FA (Bershadsky et al., 1985).

Fibronectins (FNs) are disulphide-bonded dimeric glycoproteins that consist of three types of homologous repeating modules termed I, II and III (Petersen et al., 1983). These repeats are organised into a series of functional domains that bind to integrins, collagens, heparin and FN. The tertiary structure of different type III modules within FN is similar. X-ray crystallographic studies demonstrate that each type III module consists of three or four β-strands forming a sandwich of anti-parallel β-sheets. The primary integrin-dependent cell-binding site in FN has been located in the RGD sequence of the III_{10} module. Moreover, several 'synergistic' and/or 'interacting' sites on neighbouring modules have been identified (Potts and Campbell, 1996). Diversity in FNs is due to alternative splicing in type III repeats ED-A, ED-B and IIICS (Hynes, 1990). The ED-A domain is capable of promoting cell attachment and its activity is synergised by neighbouring repeats III_{11} and III_{12} (Xia and Culp, 1994; Xia and Culp, 1995). The incorporation of the ED-A domain changes the overall conformation of the FN molecule and

enhances the accessibility of the RGD loop within the cell-binding domain or sites involved in fibril assembly (Bourdoulous et al., 1998; Johnson et al., 1999; Leahy et al., 1996; Manabe et al., 1997). Initial cell adhesion to FN is followed by cell spreading and formation of FA plaques in which FN-containing fibrils and actin filaments become aligned along the cell membrane (Singer et al., 1987). Actin filaments converge into these adhesion complexes where they associate to FN receptors, i.e. α5β1 integrin, and bind to proteins including talin, vinculin and α-actinin (Marcantonio et al., 1990). The assembly of FAs and the formation of actin stress fibers are regulated by growth-factor-inducing intracellular signals through the activation of the GTP-binding protein Rho (Ridley and Hall, 1992). Recent data indicate that the transformation of initial adhesion structures to mature FAs is due to the Rho-regulated centripetal tension exerted by actin-myosin present at the cell periphery (Bershadsky et al., 1996; Chrzanowska-Wodnicka and Burridge, 1992; Chrzanowska-Wodnicka and Burridge, 1994; Pletjushkina et al., 1998). In addition, Rho-mediated contractility plays a major role in matrix assembly by exposing cryptic sites of the FN molecule that are crucial for polymerisation (Zhong et al., 1998). It was also demonstrated that FN regulates assembly of actin filaments and focal contacts via the heparin-binding site in III_{13}, but stress fiber formation requires the presence of III_{13} and $III_{7\text{-}11}$ domains, either as a single protein or as separate polypeptides (Bloom et al., 1999).

During the transition of fibroblasts into myofibroblasts, modifications of FAs, actin cytoskeleton and extracellular matrix are closely interconnected (Serini and Gabbiani, 1999). In vivo and in vitro, this transition is promoted by transforming growth factor β (TGFβ) and is accompanied by the expression of α-smooth muscle actin (α-SMA) and of ED-A FN (Serini et al., 1998; Vaughan et al., 2000). FAs of myofibroblasts, usually described as 'fibronexuses' (Singer, 1982; Singer, 1979), are characterised by close alignment of actin bundles and FN fibers. To date, the relationship between fibronexus formation and FA maturation has not been evaluated. We have recently reported a correlation between α-SMA expression and FA elongation in rat fibroblasts cultured from various organs and tissues (Dugina et al., 1998). The aim of the present study was to determine whether the appearance and disappearance of myofibroblastic features are accompanied by changes in the organisation of FAs.

Our results show that during myofibroblast differentiation there is significant elongation of FA with the formation of complex structures presumably arising from the fusion of several FAs. We propose the term 'supermaturation' for this phenomenon. Supermature FAs are always associated with α-SMA-positive bundles and are probably dependent on the existence of tensile forces generated within and outside the cell.

MATERIALS AND METHODS

Cell culture and treatment

Human fibroblasts expressing low amounts of α-SMA were obtained from Dupuytren's nodules. Additional experiments using mouse, rat and human subcutaneous fibroblasts gave results similar to those obtained with Dupuytren's fibroblasts. Cells were cultured in Eagle's minimum essential medium (MEM; Life Technologies AG, Basel, Switzerland) containing 10% fetal calf serum (FCS; Seromed, Biochrom KG, Berlin, Germany), 100 U/ml penicillin, 100 mg/ml streptomycin and 2 mM L-glutamine at 37°C in a humid atmosphere of 5% CO_2. Cells seeded onto glass coverslips at a concentration of 2×10^4 cells in 35 mm-diameter culture dishes, in MEM supplemented with Monomed (a defined serum-free medium containing insulin, transferrin, sodium selenite, 2-mercaptoethanol, 2-aminoethanol, sodium pyruvate, glutamine and a BSA-oleic acid complex; Commonwealth Serum Laboratories, Melbourne, Australia) were cultured for 1-5 days. Passage 5-10 rat lung fibroblasts expressing high amounts of α-SMA (Dugina et al., 1998) were plated onto coverslips at a concentration of 2×10^4 cells in 35 mm-diameter culture dishes, in MEM supplemented with 10% FCS.

TGFβ2 (gift of A. Cox, Novartis, Basel, Switzerland) was used at the concentration of 5 ng/ml. Additional experiments using TGFβ1 (R&D Systems, Inc., Minneapolis, MN) gave results similar to those obtained with TGFβ2.

The following inhibitors of actin-myosin interaction were used: 2,3-butanedione-2-monoxime (BDM, Sigma Chemical Co., MO, USA), 30 μM for 3 hours, or ML-7 (Alexis Corp., Läufelfingen, Switzerland), 20 μM for 2-4 hours.

The following specific MAPK inhibitors were used: PD098059, an inhibitor of MEK-1 activation (Sigma Chemical Co.), 5-50 μM, or SB203580, an inhibitor of p38 MAP kinase/reactivating kinase (Sigma Chemical Co.), 20 μM for Dupuytren's fibroblasts and 50 μM for lung fibroblasts. Cells were maintained in serum free medium and treated with MAPK inhibitors for 4 hours before the addition of TGFβ.

Biotinylation of proteins

Recombinant FN fragments (6×His-tagged rED-A, gift of V. Koteliansky, Biogen Inc., Cambridge, MA; 6×His-tagged r11A12 and r11-12, gift of L. Zardi, National Institute for Cancer Research, Genova, Italy) were biotinylated by using a commercial kit (PIERCE, Rockford, IL) according to the manufacturer instructions. The recombinant protein at 1 mg/ml was linked to Sulfo-NHS-LC-LC-Biotin at a molar ratio of 1:3. Biotinylation was validated by slot blot using streptavidin and biotinylated horseradish peroxidase. Immunoreactivity of biotinylated rED-A and r11A12 was validated with the same procedure using IST-9 (anti-ED-A FN mAb, gift of L. Zardi) to ensure that biotinylation did not alter the properties of the molecule. We used biotinylated rED-A or control fragments at a concentration of 50-100 μg/ml, IST-9 at 300 μg/ml, ED-A-enriched cellular FN (purified from SKMEL 28 human melanoma cells, gift of L. Zardi) and plasma FN (pFN, Sigma Chemical Co.) at a concentration of 10-30 μg/ml of culture medium.

Immunofluorescence and confocal laser scanning microscopy

Cultured cells were rinsed in PBS containing 0.5 mM $CaCl_2$ and 3 mM $MgCl_2$ (PBS^{++}), and either permeabilized-fixed with 0.2% Triton X-100 in 3% paraformaldehyde in PBS for 5 minutes and then fixed in 3% paraformaldehyde in PBS for 10 minutes, or directly fixed in methanol at −20°C for 5 minutes.

We used: affinity-purified rabbit polyclonal anti-FN antibody (Sigma Chemical Co.) and mouse IgG1 mAbs selectively raised against different domains of FN splice variants (IST-4, to the fifth FN type III domain; IST-9, against ED-A FN and BC-1, against ED-B FN; gift of L. Zardi; (Borsi et al., 1987; Carnemolla et al., 1987)); DIA-900, an IgG1 mAb, against the 6×His tag (Dianova, Hamburg, Germany), anti-αSM-1, an IgG2a mAb, against α-SMA (Skalli et al., 1986); hVIN-1, an IgG1 mAb against vinculin (Sigma Chemical Co.); an IgG2b mAb against tensin, an IgG1 mAb against paxillin, an IgG1 mAb against FAK (Transduction Laboratories, Lexington, KY); SAM-1, an IgG2b mAb against α5β1 integrin (a gift of A. Sonnenberg, The Netherlands Cancer Institute, Amsterdam,

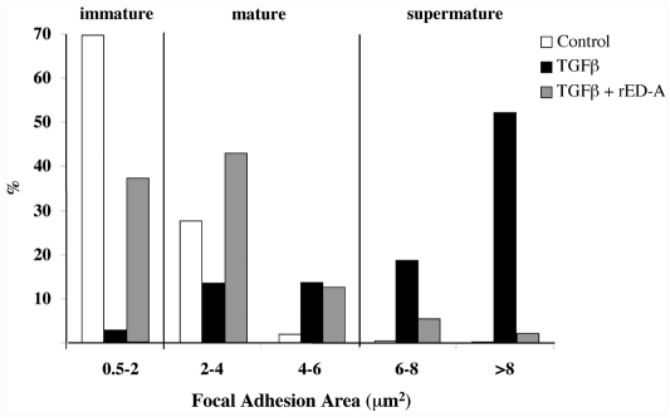

Fig. 1. Percentages of FAs showing different area in control and after treatment with TGFβ or TGFβ plus rED-A.

Netherlands); a rabbit polyclonal anti-α5β1 integrin antibody (gift of V. Belkin, Hematological Scientific Center, Moscow, Russia); and β-74, rabbit polyclonal anti-β-actin antibody (Yao et al., 1995). As secondary antibodies we used FITC- and TRITC-conjugated goat anti-mouse IgG2a, IgG2b and IgG1 (Southern Biotechnology Associates Inc., Birmingham, AL), Alexa™ 488 (Molecular Probes, Eugene, Oregon, OR)- and TRITC (Jackson Immunoresearch Laboratories, West Grove, PA)-conjugated goat anti-mouse or anti-rabbit IgG. Texas Red (Anawa, Wangen, Switzerland)- or Alexa™ 488 (Molecular Probes)-conjugated streptavidine were used for detection of biotinylated rED-A fragment. Total F-actin was stained with FITC-conjugated phalloidin (Sigma Chemical Co.) or phalloidin-Alexa™ 488 (Molecular Probes).

Double immunofluorescence-labeled cells were observed with a confocal laser scanning inverted microscope (LSM 410; Carl Zeiss, Jena, Germany) equipped with two lasers used simultaneously: a helium laser (excitation wavelength 543 nm) and an argon-neon laser (excitation wavelength 488 nm). The objectives were immersion oil plan-neofluar 63×/1.4 and 100×/1.3. Serial optical sections of individual cells were taken in a total depth of 4-6 μm with a z-step of 0.2 μm. Three-dimensional reconstructions were computed by image analysis software (IMARIS, Bitplane, Zürich, Switzerland) running on an Octane Silicon Graphics workstation (Mountain View, CA). Three-dimensional shadow and perspective projections were used for visualisation of interconnected structures.

Morphometry

Digital images were taken using a Zeiss Axiophot microscope (Carl Zeiss) equipped with an air-cooled digital 3-chip CCD red-green-blue high sensitivity camera (Photonic Science Coolview, Carl Zeiss). Images were analysed using the software KS400 (version 2.0; Kontron System, Carl Zeiss), using color thresholding program to select cells that display no cell-cell contacts, and their shape characteristics were calculated. The parameters 'area of cell projection', 'elongation' and 'dispersion' were calculated according to Dunn and Brown (1986). Elongation and dispersion have simple transformation properties and can detect fundamental transformations of cell shape. Measurement of dispersion and elongation indices is based on the assumption that cell shape is represented by a thin lamina with a uniform unit density. Both indices measure the extension of total mass of the lamina away from its center of gravity (Dunn and Brown, 1986). Elongation is invariant to scaling and dispersion is invariant to both scaling and

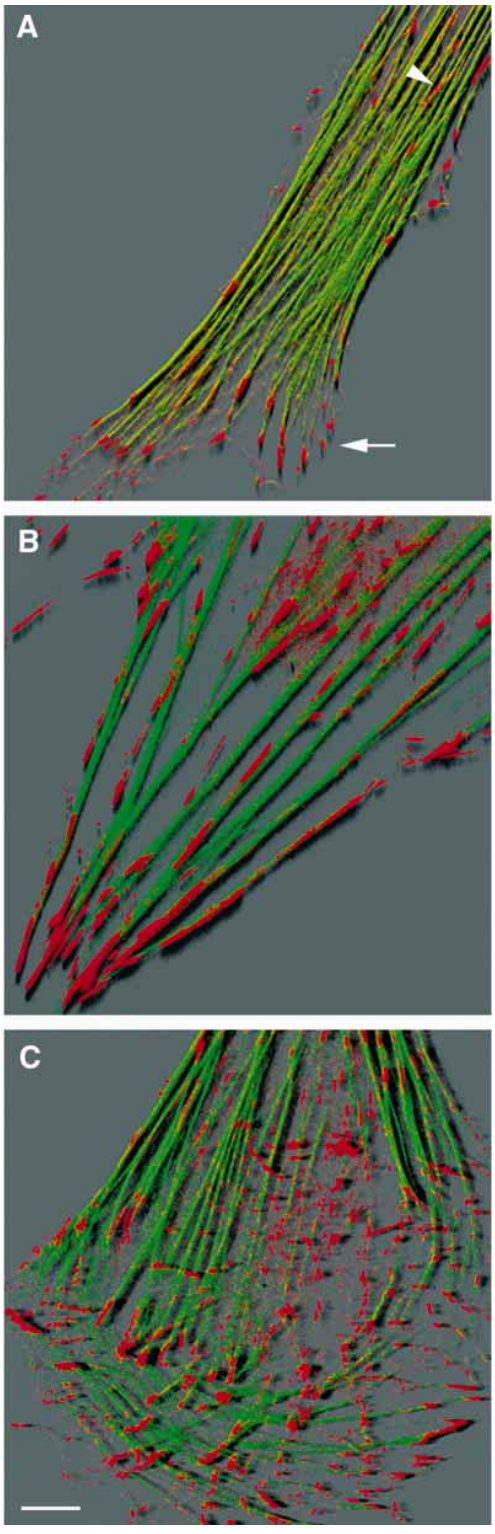

Fig. 2. Modulation of FAs and stress fiber structure after TGFβ treatment. 3D shadow projections, views from the cell basal side. (A) Vinculin (red) and β-cytoplasmic actin (green) organisation in control fibroblasts. FAs are small and some are connected with cytoplasmic actin stress fibers. Immature (arrow) and mature (arrowhead) FAs. (B) Vinculin (red) and α-SMA (green) organisation in fibroblasts treated for 5 days with TGFβ. The size of vinculin-containing FAs is dramatically increased in parallel with the appearance of α-SMA in stress fibers. (C) Vinculin (red) and β-cytoplasmic actin (green) organisation in fibroblasts after TGFβ-treatment in the presence of rED-A. FAs are smaller and stress fibers are thinner than those in B. α-SMA is absent in stress fibers. Bar, 10 μm.

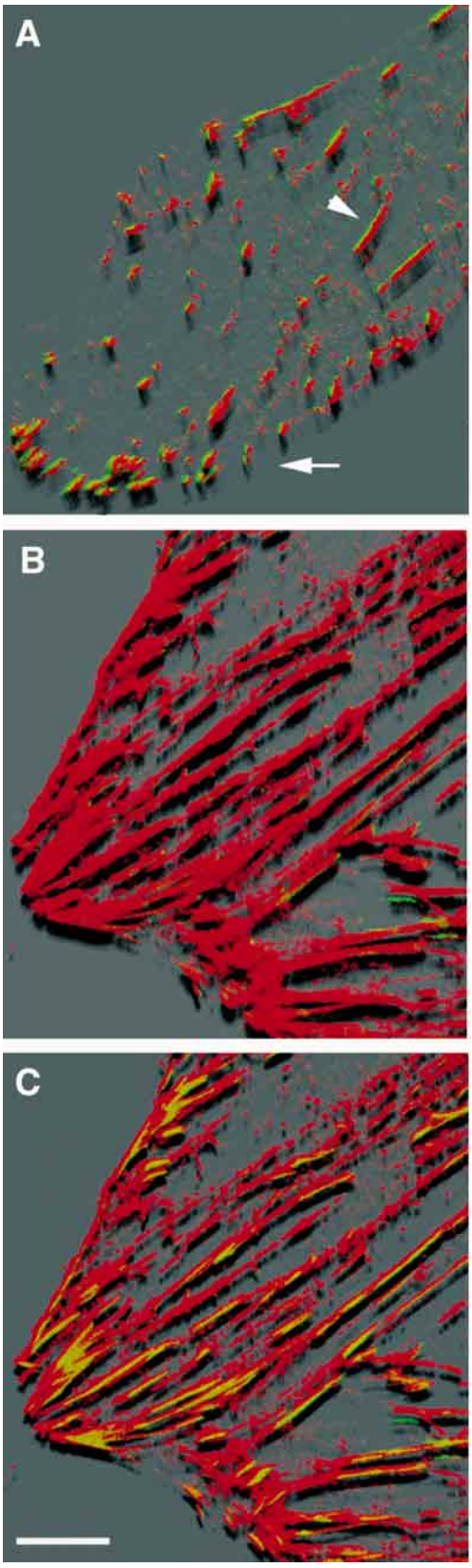

Fig. 3. Codistribution and 3D-structure (shadow projections) of vinculin and α5β1 integrin in FAs of control and TGFβ-treated fibroblasts. (A) Immature (arrow) and mature (arrowhead) FAs of a control fibroblast (view from ventral side): α5β1 integrin (red) is adjacent to vinculin (green) or colocalised with vinculin (yellow). (B,C) FAs after 5 days of TGFβ treatment. (B) Vinculin staining is hidden by α5β1 integrin staining (basal side of the cell). (C) Vinculin and α5β1 integrin co-staining (yellow) in FAs appears after removing the first basal optical sections. The terminal portions of FAs appear surrounded by α5β1 integrin. Bar, 10 μm.

stretching and hence to all transformations (Brown et al., 1989). We have designated as 'capes' evaginations of cell membrane longer than 15 μm and with a width at their base of less than 10 μm (Dugina et al., 1998). At least 50 cells from three experiments were examined in each group of experiments.

For morphometry of FAs, cells stained with anti-vinculin alone or in combination with anti-α-SM-1 were observed by confocal microscopy using oil immersion plan-neofluar 63×/1.4 objective, field was zoomed 1.5 times and optical sections of 512×512 pixels were acquired. Images were subsequently analysed using the software KS400. The length of vinculin-stained FAs was defined by their longest axis regardless of orientation. The ratio of areas of FAs/area of the corresponding cell region (always selected within the lamellar zone of the cell edge) and area of single FA were evaluated. For technical reasons the selected areas were not always the same, but there was no significant difference between the areas of the regions selected in the different experimental groups. At least 30 cells from three experiments were examined in each group.

Isolation of adherent matrices and overlay binding assay

Fibroblasts grown on glass coverslips or on 12-well plastic plates were washed three times in 1 ml of PBS^{++} then extracted three times in 100 μl of DOC buffer (50 mM Tris, pH 8.0; 10 mM EDTA, 2% (w/v) desoxycholate). The three extracts were pooled and corresponded to the DOC-soluble pool. The remaining FN matrix tightly bound to the substrate (DOC-insoluble pool) was either used directly for overlay binding assay (see below), solubilised in 300 μl of Laemmli sample buffer or processed for immunofluorescence staining.

Overlay binding assays were performed on adherent matrices isolated from cells grown on glass coverslips. DOC-resistant matrices were equilibrated in Hank's medium and nonspecific binding sites were blocked by a 30 minute incubation in the same medium containing 2 mg/ml of heat-inactivated BSA. The resulting matrices were then incubated in Hank's-BSA containing biotinylated recombinant FN fragments at 50 μg/ml for 3 hours at room temperature. Samples were washed three times in Hanks' medium, fixed for 15 minutes in 3% paraformaldehyde and processed for immunofluorescence.

SDS-PAGE and western blot analysis

Protein samples resolved by SDS-PAGE under reducing conditions on 6% gels for FN, 8% gels for cytoskeletal proteins and 12% gels for biotinylated rED-A were transferred to nitrocellulose membranes in buffer containing 25 mM Tris, 192 mM glycine, 20% methanol (vol/vol) and 0.1% SDS (w/v), pH 8.8. Membranes were then incubated with mAbs against ED-A FN, α-SMA, vinculin, paxillin; an IgG1 mAb to total actin (clone C4, Boehringer Mannheim, Germany); an IgG1 mAb against vimentin (clone V9, DAKO, Glostrup, Denmark), or the affinity-purified rabbit polyclonal anti-FN antibody. The secondary antibodies were either a goat anti-mouse IgG or goat anti-rabbit IgG conjugated with horseradish peroxidase (Jackson) and developed with ECL western blotting system (Amersham, Buckinghamshire, UK). For quantification, membranes corresponding to each western blot experiment were scanned with an Arcus II scanner (Agfa, Mortsel, Belgium) and analysed with the Image Quant Software Version 3.3 (Molecular Dynamics, Sunnyvale, CA) as previously described (Bochaton-Piallat et al., 1998).

Cytoskeleton fractionation

Adherent cells grown for 4 days at low density (<30% confluency) in

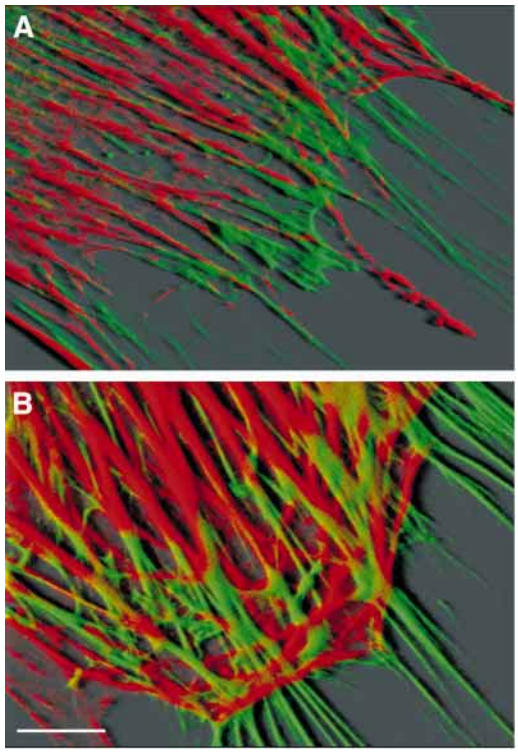

Fig. 4. Organisation of ED-A FN and actin after TGFβ treatment. 3D shadow projections. (A) β-Cytoplasmic actin (red) and ED-A FN (green) in control fibroblasts. View from basal side of the cells showing that some terminal ends of actin stress fibers are connected with FN fibers. (B) α-SMA (red) and ED-A FN (green) in fibroblasts treated with TGFβ. The appearance of α-SMA in actin stress fibers and their thickening are accompanied by an organisation of ED-A FN in parallel bundles and their association with the end of actin stress fibers. The first optical sections from basal surface of extracellular matrix adjacent to fibronexus have been removed. Bar, 10 μm.

serum-free medium were overlaid with ice-cold low-salt buffer (60 mM Pipes, 25 mM Hepes, 10 mM EGTA, 2 mM $MgCl_2$, 0.5% Triton X-100 (v/v) and 1 mM sodium orthovanadate, pH 6.9), supplemented with the cocktail of protease inhibitors Complete-EDTA (Boehringer Mannheim) and extracted for 5 minutes. The supernatant was recovered as the cytosolic TX-100 soluble fraction. This operation was repeated twice and both fractions were pooled. The material remaining tightly bound to the surface was scrapped in sample buffer and corresponded to the cytoskeletal TX-100-insoluble fraction.

RESULTS

Analysis of FA diversity and characteristic of FA categories

To analyse myofibroblastic transition we have used human fibroblasts from Dupuytren's nodules because they easily differentiate into myofibroblasts upon treatment with TGFβ (Desmoulière et al., 1993; Serini et al., 1998). They exhibited 1-5% of α-SMA-positive cells in standard culture condition and up to 80% of α-SMA positive cells after 4 days of incubation with TGFβ (Table 1). Similar results were obtained with rat, mouse and human subcutaneous fibroblasts.

When observed by phase contrast microscopy, control

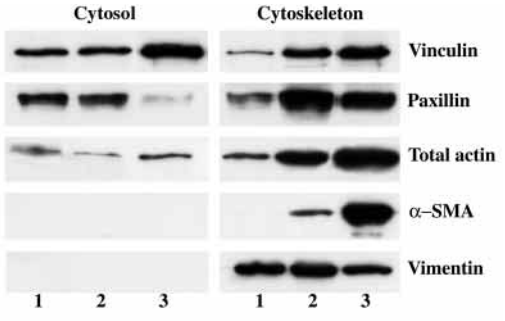

Fig. 5. Western blot analysis of cytosolic and cytoskeleton fractions prepared from fibroblasts. Control Dupuytren's fibroblasts (Lane 1) or TGFβ-treated cells (lane 2) and lung fibroblasts (Lane 3) were fractionated in cytosolic pool (left panel) and cytoskeleton pool (right panel) and probed for the presence of cytoskeletal proteins by western blot.

fibroblasts showed an elongated shape with long tails and small lamellae at the edge of the cell body (data not shown). Thin stress fibers positive for β-cytoplasmic actin were connected to several small FAs located in the lamellae at the cell edge and to few longer FAs in the central portion of the cell.

After 1 day of TGFβ incubation cells became more spread and less polarised than the corresponding controls. They had larger areas and lower elongation and dispersion indices compared with controls. The number of indentations (capes) at the cell edges was significantly higher than in control cells. After 2 days of TGFβ treatment multiple radial and tangential microfilament bundles positive for β-cytoplasmic actin were seen (data not shown). After 3 days of of TGFβ treatment β-cytoplasmic actin was organised in thick and parallel stress fibers; some of them were already positive for α-SMA. Many thin and long FAs were seen in the central part of these cells (data not shown).

After 4-5 days of treatment, TGFβ induced α-SMA expression in 60-80% of fibroblasts, which acquired a polygonal shape, significantly larger areas and decreased elongation indices compared to α-SMA-negative control (Table 1, 5 days). FAs were longer and thicker in α-SMA-positive cells than in α-SMA-negative cells. Morphometrical evaluation of lung fibroblasts having a proportion of α-SMA-positive cells of 85.0±7.2% gave similar results to α-SMA-positive fibroblasts in TGFβ-treated cultures (Dugina et al., 1998) (Table 1).

The measurements of the length and area of FAs in cells treated with TGFβ for 2 or 5 days are presented in Table 2. On the basis of these results, we arbitrarily classified FAs into three categories: immature (area ≤2 μm^2), mature (area=2-6 μm^2) and supermature (area ≥6 μm^2). Data on the distribution of these FA categories are presented in Fig. 1. The structure of immature, mature and supermature FAs was further analysed by using software for 3D-reconstruction of optical serial sections.

Immature FAs (1.60±0.45 μm in length, 0.78±0.21 μm width) were mainly present in α-SMA-negative cells of control cultures and after 1-2 days of TGFβ treatment. They appeared as small and slightly elongated structures localised near the cell edges and in the central part of lamellae (Fig. 2A). The smallest FAs were found under ruffles and were often connected with thin β-cytoplasmic actin bundles. These FAs stained for

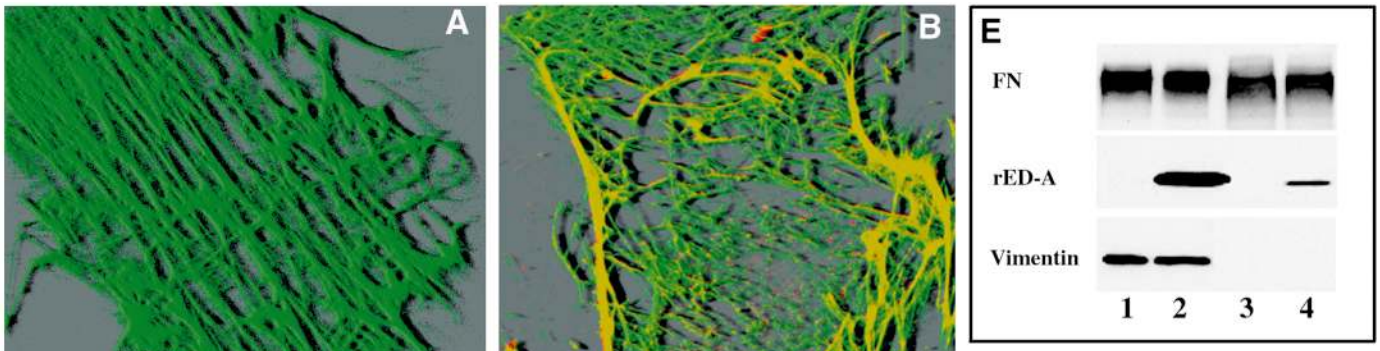

Fig. 6. Incorporation of biotinylated rED-A into the cellular FN network. 3D shadow projections, views from basal side (A,B). Single optical sections (C,D). Bar, 10 μm. (A) Fibroblasts treated with TGFβ for 4 days. ED-A FN (green) displays a parallel organisation of thick fibers. (B) TGFβ-treated fibroblasts in the presence of rED-A (red). Yellow staining shows zones of colocalisation. The organisation of the FN network is less regular upon rED-A treatment compared to TGFβ treated fibroblasts (A). Biotinylated rED-A displays a preferential incorporation into the FN network near the periphery of the cell. Note the thickening of FN fibers mainly at the places of rED-A incorporation. (C,D) Desoxycholate (DOC)-resistant matrix deposited by TGFβ-treated cells (C) or by TGFβ-treated cells incubated with biotinylated rED-A (D): rED-A (red) and ED-A FN (green). Note a focal incorporation of rED-A into the fibers of DOC-insoluble FN matrix (D). As for B, yellow staining represents zones of colocalisation. (E) DOC-soluble (lanes 1 and 2) and -insoluble (lanes 3 and 4) fractions were prepared from fibroblasts cultured for 4 days in 5 ng/ml of TGFβ in the absence (lanes 1 and 3) or in the presence of 100 μg/ml of biotinylated rED-A (lanes 2 and 4). Corresponding amounts of proteins were resolved on 6% gels (FN), 8% gels (vimentin) and 12% gels (rED-A) and probed with a rabbit polyclonal antibody to FN or streptavidin, and with a monoclonal antibody to vimentin. rED-A is incorporated in the DOC-insoluble matrix but does not reduce the level of DOC insoluble FN or of vimentin.

vinculin and paxillin; they were colocalised with short (1-2 μm in length) and thin (0.5-1 μm wide) α5β1 integrin accumulations (Fig. 3A). They were negative for tensin and FAK. Most of the actin bundles were related to thin ED-A FN-positive fibers on the outer edges of the cells (Fig. 4A).

Mature FAs (4.16±2.43 μm in length, 1.07±0.46 μm width) were found mainly in α-SMA-positive cells in control culture and in α-SMA-positive cells after 1-2 days of TGFβ treatment. They were located at the lower surface of the lamellae but not at their edge. They could be connected with α-SMA-negative or α-SMA-positive stress fibers. They were stained for vinculin, paxillin, tensin and FAK. α5β1 Integrin was localised on the ventral side of vinculin contact (Fig. 3A). These FAs were connected with parallel fibers of ED-A FN located at the basal cell surface.

Supermature FAs (16.07±6.79 μm in length, 2.77±1.48 μm in width) were observed only in α-SMA-positive cells of TGFβ-treated culture (3-5 days) and in lung fibroblasts. These

Table 1. Morphological features of cultured Dupuytren's fibroblasts after stimulation of α-SMA expression by TGFβ*

Treatment	α-SMA‡	Area (μm²)	Dispersion	Elongation
Control	+ (3.0±2.5)	5937±537	0.69±0.07	1.18±0.12
	–	3027±416	1.36±0.12	2.62±0.12
TGFβ	+ (71.0±9.6)	6242±577	0.35±0.03	1.18±0.07
	–	3101±207	0.57±0.11	2.4±0.14

*Mean±s.e. is given. At least 50 cells from three experiments were used for the calculations in each group.
‡Percentage of positive cells is shown in parentheses.

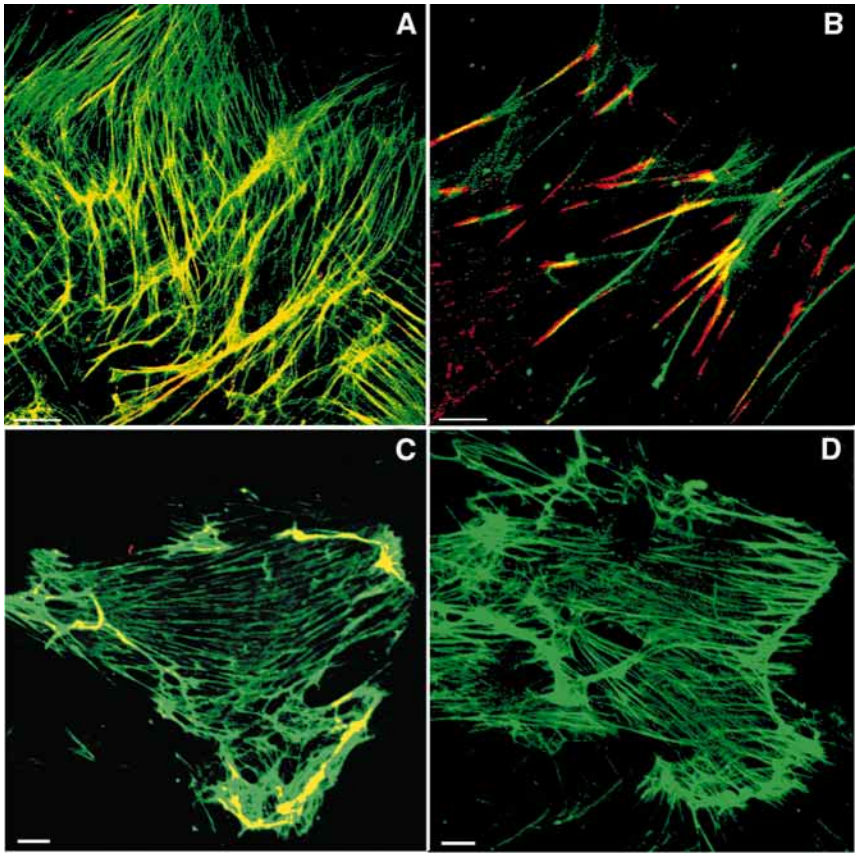

Fig. 7. Incorporation of rED-A into cellular FN fibers. Fibroblasts were cultured for 4 days in TGFβ and then for 3 hours in the presence of 50 μg/ml of biotinylated rED-A (A,B). (A) Biotinylated rED-A (red) displays a preferential incorporation (yellow) into thick fibers of the ED-A FN (green) network. (B) Vinculin (red) in FAs is partially overlapping (yellow) with rED-A (green) fibers. (C,D) Overlay binding assays: DOC-insoluble matrix prepared from TGFβ-treated fibroblasts was overlaid with biotinylated rED-A (C) or r11A12 (D) at 50 μg/ml, 3 hours. (C) rED-A (red) primarily colocalises with thick fibers of FN (green). (D) The recombinant protein r11A12 does not decorate FN fibers (green). Bars, 10 μm.

highly elongated cylindrical bodies often merged into conical structures where vinculin (Fig. 2B), paxillin, tensin and FAK surrounded the ends of α-SMA-positive actin stress fibers. Three-dimensional reconstruction revealed that in these structures integrin-positive layers alternated with vinculin-positive ones (Fig. 3B,C). The vinculin layers were often thicker and longer on the basal part of the cell than on the dorsal side. These structures were in contact with both ventral and dorsal cell membranes near the cell edge.

Three-dimensional reconstruction of ED-A FN distribution demonstrated brush-like structures on the lower and upper cell surfaces. These structures were connected with the end of thick α-SMA bundles (Fig. 4B) and with the tip of vinculin-containing FAs. They surrounded the conical edges of α5β1 integrin stripes (data not shown). In addition, the ends of actin bundles were often related to ED-A FN fibers outside the cell (Fig. 4B).

Biochemical analysis of FA-associated proteins

We employed western blots to investigate whether paxillin, vinculin and actin were enriched in the cytoskeleton fractions prepared from Dupuytren's fibroblasts, either nontreated or treated for 5 days (maximal effect) by TGFβ. Blots were normalised to vimentin, which was not affected by TGFβ treatment and was found exclusively in the cytoskeleton fractions (Fig. 5). Vinculin and paxillin were primarily in the cytosolic pool and actin in the cytoskeleton pool of nontreated cells. TGFβ increased slightly the expression of vinculin and, more importantly, the expression of paxillin and actin; moreover, it promoted the incorporation of these proteins into the cytoskeleton pool (Fig. 5). Western blot quantification indicated that upon TGFβ treatment the proportion of incorporation into the cytoskeleton pool increased from 30% to 55% for vinculin, from 40% to 70% for paxillin and from 50% to 80% for total actin. Western blot analysis performed on cytosolic and cytoskeleton extracts prepared from lung fibroblasts revealed that vimentin, vinculin, paxillin and actin were abundant in the cytoskeleton pool (Fig. 5). Scanning of western blots indicated that the proportion of incorporation into the cytoskeleton pool was 40% for vinculin, 90% for paxillin and 80% for total actin.

Effects of rED-A and IST-9 on the organisation of the FN network and on the maturation of FAs

As expected, ED-A FN expression increased dramatically in Dupuytren's fibroblasts cultured upon TGFβ treatment. A clear difference in the organisation of the FN network was observed in rED-A treated cells. Although, in TGFβ-treated cells, the FN network appeared as thick parallel fibers underneath the

Table 2. FA features in Dupuytren's fibroblasts after TGFβ treatment*

Treatment		Length (μm)	Relative area of FAs (% of selected cell region)	FA area (μm²)
Control	2 days	1.78±0.76	1.87±0.05	0.94±0.02
TGFβ		3.73±0.29	5.33±0.37	3.81±0.53
Control	5 days	2.10±0.21	3.50±0.42	1.04±0.09
TGFβ		7.91±0.76	14.21±0.63	7.92±2.32
TGFβ+rED-A		2.97±0.08	5.61±0.78	2.68±0.97

*Mean±s.e. is given. At least 30 cells from three experiments were used for the calculations in each group.

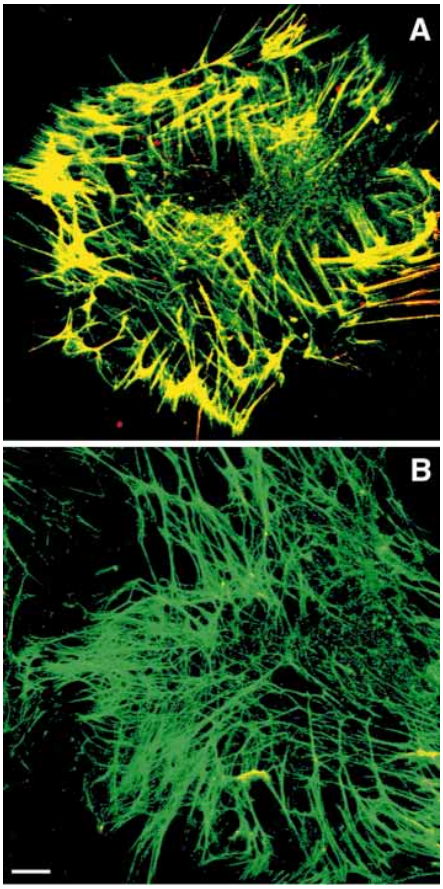

Fig. 8. Blocking of the incorporation of rED-A into cellular FN network by inhibitor of actin-myosin contractility. (A) Fibroblasts were incubated for 5 days in TGFβ, then 100 μg/ml of biotinylated rED-A was added for 3 hours. A high incorporation (yellow) of rED-A (red) into the ED-A FN network (green) is visible. (B) ML-7 added into the culture medium 1hour before and during incubation with rED-A blocks rED-A incorporation into ED-A FN. Bar, 10 μm.

ventral plasma membrane (Fig. 6A), a FN network with irregularly distributed thin fibers was visible in connection with rED-A treated cells (Fig. 6B). Double staining for biotinylated rED-A and FN revealed that rED-A fragments colocalised with the FN network preferentially near the perimeter of the cell (Fig. 6B). FN fibers were clearly thicker at the place of rED-A insertions. Interestingly, rED-A treatment of control cultures resulted in point-like incorporation of the rED-A fragment into the FN network.

As previously reported (Serini et al., 1998), rED-A reduced α-SMA expression in TGFβ-treated Dupuytren's fibroblasts. In addition, actin filaments appeared randomly oriented (Fig. 1C); moreover, FAs remained of the mature type (Fig. 1C; Table 2; Fig. 2) suggesting that rED-A inhibits FA supermaturation. In these conditions the α5β1 integrin appeared as thin streaks connected to each other and sometimes forming small conglomerates (data not shown). Treatment with the IST-9 antibody similarly inhibited FA supermaturation and collapsed the FN network into thick ribbons (data not shown).

rED-A associates with polymerised FN

To control our morphological observation, we further investigated whether biotinylated rED-A associated with the polymerised fraction of the FN matrix in TGFβ-treated fibroblasts. The staining pattern of rED-A in FN matrix was the same in DOC-nonextracted and -extracted cells (Fig. 6B,D). rED-A was colocalised with fibers of the ED-A FN within the DOC-insoluble matrix (Fig. 6D). By western blot, rED-A was abundant in the DOC-soluble and -insoluble pool (Fig. 6E, lanes 2,4, middle panel) suggesting that rED-A copolymerises with FN. We also verified whether rED-A could interfere with FN polymerisation. Western blot analysis performed on DOC-soluble and -insoluble fractions prepared from cells cultured in medium containing or not containing rED-A showed no differences in the level of polymerised FN (Fig. 6E, lanes 1-4, upper panel). Vimentin, used as control, remained unchanged upon rED-A treatment (Fig. 6E, lanes 1-4, lower panel) and was exclusively found in the DOC soluble fraction (lanes 1 and 2).

After a short period of treatment with biotinylated rED-A, rED-A-containing fibers were identified (Fig. 7A) mainly in connection with FAs (Fig. 7B). Similar pictures were obtained for FAs stained with anti-α5β1 integrin antibodies (data not shown).

We further examined whether in a cell-free system rED-A can decorate a FN matrix produced by Dupuytren's fibroblasts. DOC-insoluble matrix was prepared and overlaid with biotinylated rED-A. As shown in Fig. 7C, we found that rED-A colocalises only with thick FN fibers. Similar experiments were conducted using biotinylated recombinant FN fragment r11A12 to determine whether the ED-A domain maintains its effect when flanked by its neighbouring repeats. Neither r11A12, nor r11-12 used as control, did bind to the DOC-insoluble FN deposited by cells (Fig. 7D). This suggests that rED-A preferentially associates with FN stretched by cells at the sites of FAs. To test this hypothesis, we investigated whether the incorporation of rED-A in FN network was altered in fibroblasts treated with ML-7, an inhibitor of SM-myosin light chain kinase; rED-A incorporation was abolished in ML-7 treated cells compared with untreated cells (Fig. 8A,B)

We have also found that rED-A treatment induces strong modifications of rat lung fibroblast features in the absence of any TGFβ treatment. Upon incubation with rED-A, FN cells display thin lamellae and lamellipodia at their edges instead of the typical capes observed in control culture. Addition of rED-A leads to a reorganisation of actin network from thick and well-oriented fibers into more delicate and randomly oriented α-SMA-positive filaments. The development of FAs reached only the stage of mature contacts compared with predominance of large supermature FAs in control fibroblasts (data not shown).

Treatment with BDM or ML-7 resulted in filopodium activity and leading-edge extension in lung fibroblasts. Cell leading edges lost short spikes, which were typical of control cultures. Most of the FAs became shorter with the disappearance of α-SMA from stress fibers. Immunofluorescence staining for ED-A FN showed the disruption of FN network into thin fragments. Average length of vinculin containing FA after BDM treatment was reduced to 2.2±0.25 μm compared to 11.17±0.25 μm in control lung fibroblasts. Similarly, in ML-7 treated cells the average length of focal contact was shortened to 4.1±0.21 μm instead of the 12.26±0.5 μm measured in untreated cells.

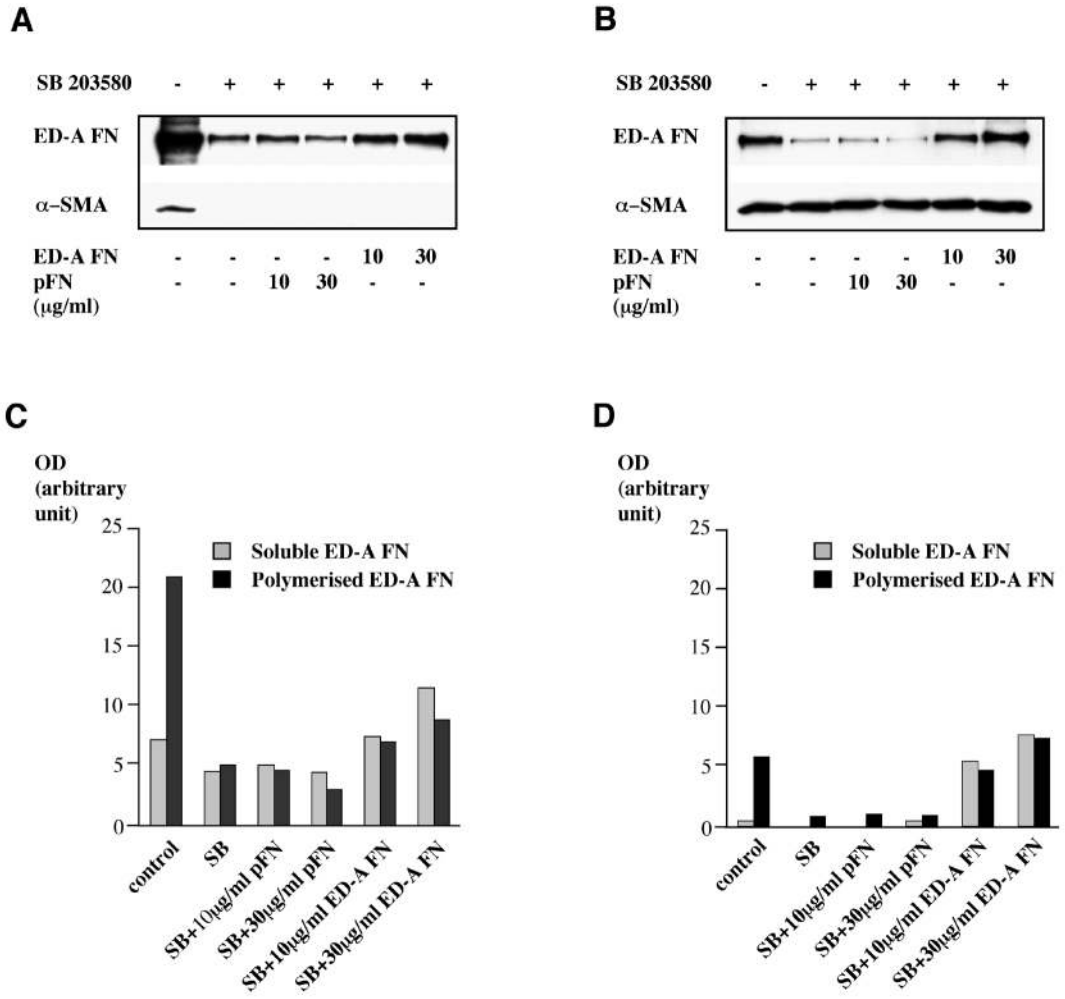

Fig. 9. Effect of MAPK inhibitor SB230580 on ED-A FN polymerisation. Dupuytren's (A,C) and lung fibroblasts (B,D) cultured in the presence of various concentration of FN and treated with 20 μM and 50 μM, respectively, of SB230580 for 4 days were either extracted by DOC to recover the polymerised FN fraction or solubilised in loading buffer. Polymerised ED-A FN was probed by western blot on DOC insoluble fraction using IST-9 antibody (A,B, upper line) and α-SMA expression tested by western blot of whole cell extracts (A,B, lower line). The production of ED-A FN by the cells was tested by dot blot analysis of culture medium using IST-9 antibody. Western and dot blots were quantified by scanning densitometry to compare the level of soluble and polymerised ED-A FN (C,D).

Action of MEK1 and p38 activation inhibitors

Finally, we tested whether inhibition of MAPKs interferes with FN polymerisation and α-SMA expression. TGFβ-treated Dupuytren's fibroblasts were incubated either with PD098059, an inhibitor of MEK1 activation, or with SB230580, an inhibitor of p38 activation. Inhibition of MEK1 had no effect on myofibroblast differentiation induced by TGFβ (not shown). By contrast, when TGFβ-treated Dupuytren's fibroblasts were pretreated with SB230580, there was a clear inhibition in the level of polymerised ED-A FN and a complete inhibition of α-SMA expression (Fig. 9A). In addition, this inhibitor reduced the level of soluble FN in the culture medium (Fig. 9C). In lung fibroblasts, SB230580 strongly reduced the polymerisation of ED-A FN but had no effect on α-SMA expression (Fig. 9B). PD098059 did not change α-SMA and ED-A FN expression in lung and Dupuytren's fibroblasts.

Because we have recently reported that ED-A FN is crucial for TGFβ-induced α-SMA expression in fibroblasts, we tested whether we could restore α-SMA expression by supplementing cell medium with either ED-A-enriched cellular FN or plasma FN. As shown in Fig. 9, in Dupuytren's fibroblasts α-SMA expression was not restored by 10 or 30 μg/ml of both FNs (Fig. 9A), although the last concentration was higher than that present in the culture medium of TGFβ-treated cells. In addition, there was a strong reduction in the level of polymerised FN (Fig. 9C). Interestingly, the level of polymerisation of ED-A FN was restored and even increased when lung fibroblasts were supplemented with either 10 or 30 μg/ml of ED-A-enriched cellular FN (Fig. 9B,D).

DISCUSSION

Myofibroblast differentiation is associated with FA modulation

Our results show that, after initiation and maturation, FAs may undergo a further reorganisation, for which we suggest the term 'supermaturation'. We show that FA supermaturation, either

Table 3. Features of different FA categories

Associated proteins	Immature (area <2 μm²)	Mature (area 2-6 μm²)	Supermature (area >6 μm²)
α-SMA (stress fibers)	–	+	+++
ED-A FN	+	++	+++
Integrin α5β1	+	++	+++
Vinculin	+	++	+++
Paxillin	+	++	+++
Tensin	–	+	+++
FAK	–	+	+++

present constitutively in lung fibroblasts or induced by TGFβ, coincides with the appearance of myofibroblastic features. In particular, supermature FAs are always associated with α-SMA-positive stress fibers. The main features distinguishing immature, mature and supermature FAs are schematically summarised in Table 3.

Prior to this study, there had been no clear information about the reorganisation of FA proteins during TGFβ-induced myofibroblastic differentiation. Here we report that the content of vinculin, paxillin and actin per cell, as well as the size of FAs, increase in TGFβ-treated fibroblasts compared to controls. By means of confocal laser scanning microscopy we have demonstrated the colocalisation of FA proteins (vinculin, paxillin, tensin, FAK) and of α5β1 integrin in supermature FAs. The ED-A FN meshwork was closely associated with the plasma membrane and to a great extent colocalised with FAs. Three-dimensional reconstruction of confocal images suggests that supermature FAs result from the association of smaller FAs. It is likely that supermaturation involves both longitudinal growth of individual contacts and their fusion with one another. Therefore, it may occur through a mechanism similar to that involved in the modulation of initial contacts into mature ones, i.e. longitudinal growth and fusion of individual structures (Pletjushkina et al., 1998).

Recently, cell-matrix contacts that differ from classical FAs have been identified and named fibrillar adhesions (Katz et al., 2000; Pankov et al., 2000; Zamir et al., 1999; Zamir et al., 2000). They are enriched in tensin, α5β1 integrin and FN, but contain low levels of paxillin, vinculin and tyrosine-phosphorylated proteins (Zamir et al., 1999). In our model, we did not see any typical fibrillar adhesions. Most of the supermature FAs contained high levels of α5β1 integrin, tensin, vinculin and paxillin and displayed a clear connection with FN. Our biochemical findings demonstrate the recruitment of vinculin, paxillin and α-SMA in the detergent-insoluble protein pool, further suggesting that FA supermaturation provides a stable connection between the cytoskeleton and the extracellular matrix. TGFβ appears to induce the bundling of ED-A FN fibers and their close association with the terminal portion of stress fibers. Our findings are in agreement with the model of tensin-dependent FN receptor translocation from FAs into and along fibrillar contacts (Pankov et al., 2000) for the initiation of FN fibrillogenesis. In this model, FAs are considered to be less dynamic than fibrillar adhesions. In addition, a recent study has shown that when FN is covalently linked to the substrate, cells assemble only 'classical' FAs (Katz et al., 2000). Taken together, these observations suggest that under our conditions, fibrillar adhesions are absent because of the stability of the extracellular matrix.

The relation of supermature FAs to the 'fibronexus' (Singer, 1979; Singer et al., 1984) deserves special mention. Fibronexus is usually regarded as a structure characteristic of myofibroblasts in vitro and in vivo (Eyden, 1993; Singer, 1979; Singer et al., 1984). It has been defined on the basis of electron-microscopic features as a very close association of FN fibers and actin microfilament bundles. Here we have characterised more precisely the fibronexus features that essentially correspond to mature and supermature FAs.

A role for ED-A FN in the maturation of FAs

Liao et al. (Liao et al., 1999) have suggested that specific amino acid sequences are involved in functional activities of ED-A FN. In addition, the ED-A FN domain has been shown to promote integrin-mediated cell adhesion (Manabe et al., 1997). In vitro studies have indicated that the ED-A segment favours an open conformation of the FN molecule by competing with a binding site involved in intramolecular folding that unmasks sites required for adhesion (Johnson et al., 1999). We have shown that rED-A associates with FN fibers (possibly stretched) and inhibits the formation of supermature FAs, which is consistent with the above observations. The recombinant protein r11A12 does not associate with FN fibers; this is probably because the binding sites for FN in the ED-A domain are hindered by the flanking repeats 11 and 12. These observations are in agreement with those reporting that in rabbit synovial cells the rED-A fragment, but not the r11A12, is capable of stimulating the production of MMP-1 (Saito et al., 1999).

The role of p38 in FN polymerisation and myofibroblast modulation

There is strong evidence that the MAPK superfamily of enzymes plays an important role in cell response to mechanical stress (Engel et al., 1999). Here we show that myofibroblastic modulation requires p38 activation, as SB203580 inhibits the expression of both α-SMA and ED-A FN. These results extend previous work showing that p38 activation is required for TGFβ-induced FN mRNA transcription (Kucich et al., 2000). In addition, we demonstrate that inhibition of p38 reduces FN polymerisation by fibroblasts. Because there is evidence that cell contractility is required for FN polymerisation (Zhong et al., 1998) it is conceivable that α-SMA expression plays a role in this effect.

Balance of actin-myosin cytoskeleton dependent tension and of extracellular matrix resistance in supermaturation of FAs

Previous work (Bershadsky et al., 1996; Chrzanowska-Wodnicka and Burridge, 1996; Pletjushkina et al., 1998) has

shown that actin-myosin-based cell contractility plays a crucial role in the transformation of initial contacts into mature ones. The present work suggests that the increase in cytoskeleton-dependent tension, as well as the mechanical resistance of the FN network to this tension, are essential for supermaturation of FAs. In this context, Choquet et al. (Choquet et al., 1997) have reported that FN-coated beads placed on the dorsal surface of fibroblasts respond to a restraining tension by localised strengthening of cytoskeletal linkages, allowing stronger force to be exerted. It is conceivable that the growing resistance of the FN network associated with the cell surface leads to strengthening of cytoskeleton-matrix linkages. This possibility is supported by data indicating that fibroblasts develop more elongated and stable FAs on the rigid substrata than on the flexible ones (Pelham and Wang, 1997). In our experiments, inhibition of supermaturation was provoked by rED-A treatment and by reducing actin-myosin-mediated contractility. Thus, the final state of FA appears to be determined by a balance of actin-myosin-mediated tension and of extracellular matrix resistance.

The role of the myofibroblast in producing isometric tension within granulation tissue in vivo as well as in cultured fibroblasts is presently well accepted (Serini and Gabbiani, 1999). This tension is essentially exerted at the level of FAs, which represent the connecting points between cell and extracellular matrix. We show here that upon TGFβ stimulation FAs acquire morphological and biochemical features that make them suited to allow the transmission of tension from the cell to the extracellular matrix and vice versa. Our results contribute to a better understanding of the mechanism through which the myofibroblast produces and maintains contractile force during wound healing and fibrocontractive diseases and may be useful in the planification of pharmacological strategies in view of influencing the evolution of these pathological situations.

We are grateful to A. Cox (Novartis, Basel, Switzerland) for providing recombinant human TGFβ2; L. Zardi (National Institute for Cancer Research, Genova, Italy) and V. Koteliansky (Biogen Inc., Cambridge, MA, USA) for recombinant FN fragments and antibodies against different domains of FN isoforms; A. Sonnenberg (The Netherlands Cancer Institute, Amsterdam, Netherlands) and V. Belkin (Hematological Scientific Center, Moscow, Russia) for antibodies against α5β1 integrin; G. Benzonana for preparation of antibodies and biotinylation of FN fragments; G. Celetta, A. Geinoz, A. Maurer-Hiltbrunner and P. Ropraz for technical assistance; K. Grandchamps for image analysis; and J. C. Rumbeli and E. Denkinger for photographic work. We thank M.-L. Bochaton-Piallat, S. Clément, B. Hinz and G. Serini for help and consultations. This work was executed with the help of the INTAS Grant-97-0931 and was also supported by the Swiss National Science Foundation (Grants 31-61336.00 and 31-54048.98).

REFERENCES

Bershadsky, A. D., Tint, I. S., Neyfakh, A. A., Jr and Vasiliev, J. M. (1985). Focal contacts of normal and RSV-transformed quail cells. Hypothesis of the transformation-induced deficient maturation of focal contacts. *Exp. Cell Res.* **158**, 433-444.

Bershadsky, A., Chausovsky, A., Becker, E., Lyubimova, A. and Geiger, B. (1996). Involvement of microtubules in the control of adhesion-dependent signal transduction. *Curr. Biol.* **6**, 1279-1289.

Bloom, L., Ingham, K. C. and Hynes, R. O. (1999). Fibronectin regulates assembly of actin filaments and focal contacts in cultured cells via the heparin-binding site in repeat III13. *Mol. Biol. Cell* **10**, 1521-1536.

Bochaton-Piallat, M. L., Gabbiani, G. and Pepper, M. S. (1998). Plasminogen activator expression in rat arterial smooth muscle cells depends on their phenotype and is modulated by cytokines. *Circ. Res.* **82**, 1086-1093.

Borsi, L., Carnemolla, B., Castellani, P., Rosellini, C., Vecchio, D., Allemanni, G., Chang, S. E., Taylor-Papadimitriou, J., Pande, H. and Zardi, L. (1987). Monoclonal antibodies in the analysis of fibronectin isoforms generated by alternative splicing of mRNA precursors in normal and transformed human cells. *J. Cell Biol.* **104**, 595-600.

Bourdoulous, S., Orend, G., MacKenna, D. A., Pasqualini, R. and Ruoslahti, E. (1998). Fibronectin matrix regulates activation of RHO and CDC42 GTPases and cell cycle progression. *J. Cell Biol.* **143**, 267-276.

Brown, A. F., Dugina, V., Dunn, G. A. and Vasiliev, J. M. (1989). A quantitative analysis of alterations in the shape of cultured fibroblasts induced by tumour-promoting phorbol ester. *Cell Biol. Int. Rep.* **13**, 357-366.

Carnemolla, B., Borsi, L., Zardi, L., Owens, R. J. and Baralle, F. E. (1987). Localization of the cellular-fibronectin-specific epitope recognized by the monoclonal antibody IST-9 using fusion proteins expressed in E. coli. *FEBS Lett.* **215**, 269-273.

Choquet, D., Felsenfeld, D. P. and Sheetz, M. P. (1997). Extracellular matrix rigidity causes strengthening of integrin-cytoskeleton linkages. *Cell* **88**, 39-48.

Chrzanowska-Wodnicka, M. and Burridge, K. (1992). Rho, rac and the actin cytoskeleton. *Bioessays* **14**, 777-778.

Chrzanowska-Wodnicka, M. and Burridge, K. (1994). Tyrosine phosphorylation is involved in reorganization of the actin cytoskeleton in response to serum or LPA stimulation. *J. Cell Sci.* **107**, 3643-3654.

Chrzanowska-Wodnicka, M. and Burridge, K. (1996). Rho-stimulated contractility drives the formation of stress fibers and focal adhesions. *J. Cell Biol.* **133**, 1403-1415.

Critchley, D. R. (2000). Focal adhesions - the cytoskeletal connection. *Curr. Opin. Cell Biol.* **12**, 133-139.

Desmoulière, A., Geinoz, A., Gabbiani, F. and Gabbiani, G. (1993). Transforming growth factor-beta 1 induces alpha-smooth muscle actin expression in granulation tissue myofibroblasts and in quiescent and growing cultured fibroblasts. *J. Cell Biol.* **122**, 103-111.

Dugina, V., Alexandrova, A., Chaponnier, C., Vasiliev, J. and Gabbiani, G. (1998). Rat fibroblasts cultured from various organs exhibit differences in alpha-smooth muscle actin expression, cytoskeletal pattern, and adhesive structure organization. *Exp. Cell Res.* **238**, 481-490.

Dunn, G. A. and Brown, A. F. (1986). Alignment of fibroblasts on grooved surfaces described by a simple geometric transformation. *J. Cell Sci.* **83**, 313-340.

Engel, M. E., McDonnell, M. A., Law, B. K. and Moses, H. L. (1999). Interdependent SMAD and JNK signaling in transforming growth factor-beta-mediated transcription. *J. Biol. Chem.* **274**, 37413-37420.

Eyden, B. P. (1993). Brief review of the fibronexus and its significance for myofibroblastic differentiation and tumor diagnosis. *Ultrastruct. Pathol.* **17**, 611-622.

Geiger, B., Yehuda-Levenberg, S. and Bershadsky, A. D. (1995). Molecular interactions in the submembrane plaque of cell-cell and cell-matrix adhesions. *Acta Anat.* **154**, 46-62.

Hynes, R. O. (1990). Fibronectins. In *Springer's Series in Molecular Biology*, (ed. A. Rich), pp. 546. New York: Springer-Verlag.

Izzard, C. S. (1988). A precursor of the focal contact in cultured fibroblasts. *Cell Motil. Cytoskeleton* **10**, 137-142.

Izzard, C. S. and Lochner, L. R. (1980). Formation of cell-to-substrate contacts during fibroblast motility: an interference-reflexion study. *J. Cell Sci.* **42**, 81-116.

Izzard, S. L. and Izzard, C. S. (1987). Actin-associated proteins related to focal and close cell-substrate contacts in murine fibroblasts. *Exp. Cell Res.* **170**, 214-227.

Jockusch, B. M., Bubeck, P., Giehl, K., Kroemker, M., Moschner, J., Rothkegel, M., Rudiger, M., Schluter, K., Stanke, G. and Winkler, J. (1995). The molecular architecture of focal adhesions. *Annu. Rev. Cell Dev. Biol.* **11**, 379-416.

Johnson, K. J., Sage, H., Briscoe, G. and Erickson, H. P. (1999). The compact conformation of fibronectin is determined by intramolecular ionic interactions. *J. Biol. Chem.* **274**, 15473-15479.

Katz, B. Z., Zamir, E., Bershadsky, A., Kam, Z., Yamada, K. M. and Geiger, B. (2000). Physical state of the extracellular matrix regulates the

structure and molecular composition of cell-matrix adhesions. *Mol. Biol. Cell* **11**, 1047-1060.

Kucich, U., Rosenbloom, J. C., Shen, G., Abrams, W. R., Hamilton, A. D., Sebti, S. M. and Rosenbloom, J. (2000). TGF-beta1 stimulation of fibronectin transcription in cultured human lung fibroblasts requires active geranylgeranyl transferase I, phosphatidylcholine-specific phospholipase C, protein kinase C-delta, and p38, but not erk1/erk2. *Arch. Biochem. Biophys.* **374**, 313-324.

Leahy, D. J., Aukhil, I. and Erickson, H. P. (1996). 2.0 A crystal structure of a four-domain segment of human fibronectin encompassing the RGD loop and synergy region. *Cell* **84**, 155-164.

Liao, Y. F., Wieder, K. G., Classen, J. M. and Van De Water, L. (1999). Identification of two amino acids within the EIIIA (ED-A) segment of fibronectin constituting the epitope for two function-blocking monoclonal antibodies. *J. Biol. Chem.* **274**, 17876-17884.

Manabe, R., Ohe, N., Maeda, T., Fukuda, T. and Sekiguchi, K. (1997). Modulation of cell-adhesive activity of fibronectin by the alternatively spliced EDA segment. *J. Cell Biol.* **139**, 295-307.

Marcantonio, E. E., Guan, J. L., Trevithick, J. E. and Hynes, R. O. (1990). Mapping of the functional determinants of the integrin beta 1 cytoplasmic domain by site-directed mutagenesis. *Cell Regul.* **1**, 597-604.

Pankov, R., Cukierman, E., Katz, B. Z., Matsumoto, K., Lin, D. C., Lin, S., Hahn, C. and Yamada, K. M. (2000). Integrin dynamics and matrix assembly: tensin-dependent translocation of alpha(5)beta(1) integrins promotes early fibronectin fibrillogenesis. *J. Cell Biol.* **148**, 1075-1090.

Pelham, R. J., Jr and Wang, Y. (1997). Cell locomotion and focal adhesions are regulated by substrate flexibility. *Proc. Natl. Acad. Sci. USA* **94**, 13661-13665.

Petersen, T. E., Thogersen, H. C., Skorstengaard, K., Vibe-Pedersen, K., Sahl, P., Sottrup-Jensen, L. and Magnusson, S. (1983). Partial primary structure of bovine plasma fibronectin: three types of internal homology. *Proc. Natl. Acad. Sci. USA* **80**, 137-141.

Pletjushkina, O. J., Belkin, A. M., Ivanova, O. J., Oliver, T., Vasiliev, J. M. and Jacobson, K. (1998). Maturation of cell-substratum focal adhesions induced by depolymerization of microtubules is mediated by increased cortical tension. *Cell Adhes. Commun.* **5**, 121-135.

Potts, J. R. and Campbell, I. D. (1996). Structure and function of fibronectin modules. *Matrix Biol.* **15**, 313-321.

Ridley, A. J. and Hall, A. (1992). The small GTP-binding protein rho regulates the assembly of focal adhesions and actin stress fibers in response to growth factors. *Cell* **70**, 389-399.

Saito, S., Yamaji, N., Yasunaga, K., Saito, T., Matsumoto, S., Katoh, M., Kobayashi, S. and Masuho, Y. (1999). The fibronectin extra domain A activates matrix metalloproteinase gene expression by an interleukin-1-dependent mechanism. *J. Biol. Chem.* **274**, 30756-30763.

Serini, G. and Gabbiani, G. (1999). Mechanisms of myofibroblast activity and phenotypic modulation. *Exp. Cell Res.* **250**, 273-283.

Serini, G., Bochaton-Piallat, M. L., Ropraz, P., Geinoz, A., Borsi, L., Zardi, L. and Gabbiani, G. (1998). The fibronectin domain ED-A is crucial for myofibroblastic phenotype induction by transforming growth factor-beta1. *J. Cell Biol.* **142**, 873-881.

Singer, I. I. (1979). The fibronexus: a transmembrane association of fibronectin-containing fibers and bundles of 5 nm microfilaments in hamster and human fibroblasts. *Cell* **16**, 675-685.

Singer, I. I. (1982). Fibronexus formation is an early event during fibronectin-induced restoration of more normal morphology and substrate adhesion patterns in transformed hamster fibroblasts. *J. Cell Sci.* **56**, 1-20.

Singer, I. I., Kawka, D. W., Kazazis, D. M. and Clark, R. A. (1984). In vivo co-distribution of fibronectin and actin fibers in granulation tissue: immunofluorescence and electron microscope studies of the fibronexus at the myofibroblast surface. *J. Cell Biol.* **98**, 2091-2106.

Singer, I. I, Kawka, D. W., Scott, S., Mumford, R. A. and Lark, M. W. (1987). The fibronectin cell attachment sequence Arg-Gly-Asp-Ser promotes focal contact formation during early fibroblast attachment and spreading. *J. Cell Biol.* **104**, 573-584.

Skalli, O., Ropraz, P., Trzeciak, A., Benzonana, G., Gillessen, D. and Gabbiani, G. (1986). A monoclonal antibody against alpha-smooth muscle actin: a new probe for smooth muscle differentiation. *J. Cell Biol.* **103**, 2787-2796.

Vaughan, M. B., Howard, E. W. and Tomasek, J. J. (2000). Transforming growth factor-beta1 promotes the morphological and functional differentiation of the myofibroblast. *Exp. Cell Res.* **257**, 180-189.

Xia, P. and Culp, L. A. (1994). Adhesion activity in fibronectin's alternatively spliced domain EDa (EIIIA) and its neighboring type III repeats: oncogene-dependent regulation. *Exp. Cell Res.* **213**, 253-265.

Xia, P. and Culp, L. A. (1995). Adhesion activity in fibronectin's alternatively spliced domain EDa (EIIIA): complementarity to plasma fibronectin functions. *Exp. Cell Res.* **217**, 517-527.

Yamada, K. M. and Geiger, B. (1997). Molecular interactions in cell adhesion complexes. *Curr. Opin. Cell Biol.* **9**, 76-85.

Yao, X., Chaponnier, C., Gabbiani, G. and Forte, J. G. (1995). Polarized distribution of actin isoforms in gastric parietal cells. *Mol. Biol. Cell* **6**, 541-557.

Zamir, E., Katz, B. Z., Aota, S., Yamada, K. M., Geiger, B. and Kam, Z. (1999). Molecular diversity of cell-matrix adhesions. *J. Cell Sci.* **112**, 1655-1669.

Zamir, E., Katz, M., Posen, Y., Erez, N., Yamada, K. M., Katz, B. Z., Lin, S., Lin, D. C., Bershadsky, A., Kam, Z. et al. (2000). Dynamics and segregation of cell-matrix adhesions in cultured fibroblasts. *Nat. Cell Biol.* **2**, 191-196.

Zhong, C., Chrzanowska-Wodnicka, M., Brown, J., Shaub, A., Belkin, A. M. and Burridge, K. (1998). Rho-mediated contractility exposes a cryptic site in fibronectin and induces fibronectin matrix assembly. *J. Cell Biol.* **141**, 539-551.